PERIÓDICO TCHÊ QUÍMICA
ARTIGO ORIGINAL

ESTIMAÇÃO DE PARÂMETROS DE CÉLULAS / MÓDULOS FOTOVOLTAICOS USANDO UM ALGORITMO DE EVOLUÇÃO DIFERENCIAL ADAPTATIVO TRIANGULAR

ESTIMATING OF PHOTOVOLTAIC CELLS/MODULES PARAMETERS USING A TRIANGULAR ADAPTIVE DIFFERENTIAL EVOLUTION ALGORITHM

ESTIMASI PARAMETER SEL/MODUL FOTOVOLTAIK MENGGUNAKAN ALGORITMA EVOLUSI DIFERENSIAL ADAPTIF SEGITIGA

HIENDRO, Ayong[1*]; YUSUF, Ismail[2]; JUNAIDI[3]; ERWAN, Komala[4]

[1,2,3,4] Tanjungpura University, Faculty of Engineering, Department of Electrical Engineering. Indonesia.

** Corresponding author*
e-mail: ayong.hiendro@ee.untan.ac.id

Received 03 February 2021; received in revised form 17 February 2021; accepted 28 February 2021

RESUMO

Introdução: Os sistemas fotovoltaicos (PV) se tornaram uma tecnologia de energia renovável promissora para fontes de eletricidade. A estimativa de parâmetro PV desempenha um papel vital na modelagem de sistemas PV. Embora muitos algoritmos de otimização tenham sido apresentados para obter parâmetros de PV, ainda é um desafio investigar algoritmos de alto desempenho. **Objetivo:** Este estudo teve como objetivo propor um algoritmo de evolução diferencial adaptativa triangular (TADE) para fornecer uma estimativa precisa dos parâmetros de PV. **Metodos:** Célula PV RTC-France, módulo PV Photowatt-PWP 201 e módulo PV KC200GT foram usados como estudos de caso usando modelos de circuito de diodo. O erro quadrático médio (RMSE) entre os dados medidos e estimados foi adotado para definir as funções objetivo dos parâmetros de PV. Um teste de Friedman foi usado para avaliar a confiabilidade dos algoritmos. Os resultados da estimativa dos parâmetros foram verificados para confirmar a precisão dos desempenhos do algoritmo TADE. O módulo PV operando em várias condições climáticas também foi realizado para avaliar o algoritmo TADE. **Resultados e Discussão**: Os resultados verificaram que na maioria dos casos o algoritmo TADE superou outros algoritmos de otimização de última geração. Para o modelo de diodo duplo, o algoritmo TADE obteve os parâmetros da célula PV RTC-France com o valor RMSE de 9,8243x10^{-04}, o mais preciso de todos os algoritmos. Os resultados experimentais também mostraram que o algoritmo TADE apresentou excelente capacidade e precisão na descoberta dos parâmetros PV e forneceu as melhores estimativas para dados experimentais I-V e P-V de células e módulos PV reais.. **Conclusões:** Os resultados comprovaram que o algoritmo TADE tem um ótimo desempenho em termos de precisão, confiabilidade e velocidade de convergência para estimativa de parâmetros PV, mesmo em diferentes condições climáticas.

Palavras-chave: *convergência; curva corrente-tensão; modelo de diodo duplo; raiz quadrada média do erro; modelo de diodo único.*

ABSTRACT

Background: Photovoltaic (PV) systems have become a promising renewable energy technology for electricity sources. The PV parameter estimation plays a vital role in modeling PV systems. Even though many optimization algorithms have been presented to obtain PV parameters, it is still challenging to investigate high-performance algorithms. **Aim:** This study aimed to propose a triangular adaptive differential evolution (TADE) algorithm to give a precise estimate of PV parameters. **Methods:** RTC-France PV cell, Photowatt-PWP 201 PV module, and KC200GT PV module were used as the case studies by using diode circuit models. The root mean square error (RMSE) between measured and estimated data was adopted to define PV parameter objective functions. A Friedman test was used to assess the reliability of algorithms. The parameter estimation results were cross-checked to confirm the accuracy of TADE algorithm performances. The PV module operating under various weather conditions was also performed to evaluate the TADE algorithm. **Results and Discussion**: The results verified that in most of the cases, the TADE algorithm surpassed other state-of-the-art optimization algorithms. For the double-diode model, the TADE algorithm obtained the RTC-France PV cell parameters with the *RMSE* value of 9.8243x10^{-04}, the most accurate of all algorithms. Experimental results also showed that the TADE algorithm presented an excellent capability and accuracy in discovering the PV parameters and provided the best estimates for *I-V* and *P-V* experimental data of real PV cells and modules. **Conclusions:** The results have

proven that the TADE algorithm has a great performance in terms of accuracy, reliability, and convergence speed for estimating PV parameters, even in different weather conditions.

Keywords: *convergence; current-voltage curve; double-diode model; root mean square error; single-diode model*.

ABSTRAK

Latar Belakang: Sistem fotovoltaik (PV) telah menjadi teknologi energi terbarukan yang menjanjikan sebagai sumber listrik. Estimasi parameter PV memainkan peran penting dalam pemodelan sistem PV. Meskipun telah banyak algoritma optimisasi telah dihadirkan untuk mendapatkan parameter PV, namun masih menantang untuk menemukan algoritma berkinerja tinggi. **Tujuan:** Penelitian ini bertujuan untuk mengusulkan algoritma evolusi diferensial adaptif segitiga (TADE) guna memberikan hasil estimasi yang teliti dari parameter PV. **Metode:** Sel PV RTC-France, modul PV Photowatt-PWP 201, dan modul PV KC200GT digunakan sebagai studi kasus dengan menggunakan model rangkaian dioda. Akar kuadrat rata-rata galat (RMSE) antara data yang diukur dan yang diperkirakan diadopsi untuk menentukan fungsi tujuan parameter PV. Tes Friedman digunakan untuk menilai reliabilitas algoritma. Hasil estimasi parameter diperiksa silang untuk memastikan keakuratan performa algoritma TADE. Modul PV yang beroperasi dalam berbagai kondisi cuaca juga dilakukan untuk mengevaluasi algoritma TADE. **Hasil dan Diskusi:** Hasil membuktikan bahwa di sebagian besar kasus, algoritma TADE melampaui algoritma optimisasi canggih lainnya. Untuk model dioda-ganda, algoritma TADE memperoleh parameter sel PV RTC-France dengan nilai *RMSE* = 9.8243×10^{-04}, hasil yang paling akurat dari semua algoritma. Hasil eksperimen juga menunjukkan bahwa algoritma TADE memberikan kemampuan dan akurasi yang sangat baik dalam menemukan parameter PV dan memberikan estimasi terbaik untuk data eksperimen *I-V* dan *P-V* sel dan modul PV. **Kesimpulan:** Hasil penelitian telah membuktikan bahwa algoritma TADE memiliki performa yang bagus dalam hal akurasi, reliabilitas, dan kecepatan konvergensi untuk mengestimasi parameter PV, bahkan dalam beragam kondisi cuaca.

Kata kunci: *konvergensi; kurva arus-tegangan; model dioda-ganda; galat akar rata-rata kuadrat; model dioda-tunggal.*

1. INTRODUCTION:

An accurate estimation of photovoltaic (PV) parameter values is very important to the design and performance assessment of PV systems. These parameters consist of photogenerated current, saturation current, diode ideality factor, and series and shunt resistances (Anani and Ibrahim, 2020).

The PV cells and modules are generally characterized by current (*I*)-voltage (*V*) and power (*P*)-voltage (*V*) curves. The PV parameters affect the *I-V* and *P-V* behavior of PV cells and modules, which change in electrical voltage, current, and power due to solar irradiance and temperature variations. As the output power of the PV cells and modules is dependent on solar irradiance and temperature, with knowing the PV parameters, engineers can design appropriate PV systems to operate under a variety of atmospheric conditions. It is also useful for the maintenance and monitoring operation of PV systems (Bosman *et al.*, 2020) and testing maximum power point tracking (MPPT) algorithms (Motahhir *et al.*, 2018) under various conditions and control of PV systems (Jordehi, 2016a).

The current-voltage curve of PV cells exhibits nonlinear and multivariable characteristics. The power delivered by PV cells and modules is the product of current and voltage. The *P-V* curve is obtained by multiplicating current and voltage, point for point, for all currents and voltages from open-circuit to short-circuit conditions. The estimation of the *I-V* and *P-V* curves can be conducted using online and offline measuring methods. The advantage of online measurement is its ability to measure real *I-V* and *P-V* characteristics based on site-specific conditions. However, the online measuring method is costly and requires long-term continuous monitoring (Zhu *et al.*, 2017).

On the other hand, the offline measurement for determining *I-V* and *P-V* curves is fast and accurate but cannot diagnose faults in PV systems. Therefore, PV cell models are necessary to extract the *I-V* and *P-V* characteristics offline. There are two PV cell models widely employed to represent the current-voltage relationship, such as the single-diode model (SDM) (Muhammadsharif *et al.*, 2019; Arabshahi *et al.*, 2020) and the double-diode model (DDM) (Khotbehsara and Shahhoseini, 2018). The SDM has five unknown parameters, while the DDM contained seven parameters to be estimated. The SDM is usually used in the estimation of PV parameters because of its simplicity. Yet, the DDM is considered to be more

accurate than the SDM, particularly in a low solar irradiance condition. The DDM also requires a longer running time than the SDM to perform the computational process (Abbassi *et al.*, 2019). However, both SDM and DDM need detailed information of all unknown parameters, which is generally not given by PV manufacturers. Besides, PV manufacturers still do not introduce any methods of extracting the PV parameters.

Many methods have been evolved to compute the PV parameters from the models. There are three techniques generally utilized to optimize the PV parameters, namely: analytical, numerical, and algorithmic through metaheuristics. The analytical approach is practically possible for solving the PV parameters problem. The analytical method has fast computation speed and gives relatively accurate results. However, the analytical method becomes very difficult and requires too much computational time to solve complex and large-sized problems. The analytical method has been used to compute PV parameters, such as Padé approximant (Lun *et al.*, 2013a), Taylor's Series Expansion (Lun *et al.*, 2013b), and Lambert W-function (Gao *et al.*, 2016; Chen *et al.*, 2018a). The numerical method is usually more accurate than the analytical process because it employed all the *I-V* curve points. The numerical method based on the Newton-Raphson iteration (Ghani *et al.*, 2014; Rodrigues *et al.*, 2018) or Gauss-Seidel (Et-torabi *et al.*, 2017) may converge to optimal values. The drawbacks of the numerical method that it needs extensive computational resources and will be susceptible to being nonconvergent if the search space is not convex. In order to overcome these inconveniences, metaheuristics algorithms have been developed to optimize the PV parameters. The metaheuristics algorithms have attracted more and more attention among the computational methods due to their effectiveness in solving complex problems. In the metaheuristic algorithms, the objective function and constraints do not rely on strict convexity, continuity, and differentiability. Moreover, the metaheuristic algorithms have better performance than numerical and analytical methods concerning accuracy, reliability, and convergence speed (Pillai and Rajasekar, 2018). Along with the development of the metaheuristic algorithms, they have been popular in determining the PV parameters for the last decade, for instance, Genetic Algorithm (GA) (Ismail *et al.*, 2013), Differential Evolution (DE) (Yang *et al.*, 2013), Particle Swarm Optimization (PSO) (Soon and Low, 2012), and Simulated Annealing (SA) (El-Naggar *et al.*, 2012). Other recent metaheuristic algorithms working on estimating the PV parameters are Supply-Demand-Based Optimization (SDO) (Xiong *et al.*, 2019), Chaotic Optimization Approach (COA) (Ćalasan *et al.*, 2019), Symbiotic Organisms Search (SOS) (Xiong *et al.*, 2018), and population classification evolution (PCE) (Zhang *et al.*, 2016).

Every algorithm has its own advantages and disadvantages. GA has the ability to avoid being trapped in the local optimum because it searches from parallel points. However, GA has a slow convergence process. DE is robust, but it requires the appropriate parameter settings to ensure the success of the algorithm. On the other hand, PSO is fast, but it is easy to fall into the local optimum in high-dimensional space. SA is known for its flexibility and ability to approach global optimum, but it needs much computational effort. For this reason, a single metaheuristic algorithm can be modified to improve its performance as in (Lin *et al.*, 2017; Yu *et al.*, 2017a; Chen *et al.*, 2018b; Kang *et al.*, 2018; Gao *et al.*, 2018; Li *et al.*, 2019a; Yu *et al.*, 2019; Chen *et al.*, 2019a; Pourmousa *et al.*, 2019; Liao *et al.*, 2020;). Another way to enhance the metaheuristic algorithm performance is hybridization with other algorithms as in (Jordehi, 2016b; Oliva *et al.*, 2017; Chen *et al.*, 2017; Yu *et al.*, 2017b; Beigi and Maroosi, 2018; Li *et al.*, 2019b; Chen *et al.*, 2019b; Chen *et al.*, 2019c; Long *et al.*, 2020). More often, two or more other metaheuristic algorithms are combined to create a single hybrid one. Hybridization is usually done to incorporate each of the desired features so that the overall algorithm becomes better than the single algorithm. It must be noted that a particular algorithm cannot very successfully deal with all problems. The algorithm may be very effective at solving one engineering problem, but it does not mean that the algorithm will also successfully deal with other engineering problems. For this reason, researchers utilize various kinds of algorithms to determine the most suitable one to solve a problem.

The objective function of the PV parameter optimization problem is conducted to minimize the difference between experimental and estimated data, which is stated as the root mean square error (*RMSE*). The *RMSE* has been commonly used as a standard statistical parameter to measure the performance of metaheuristic algorithms. However, the *RMSE* results reported by many metaheuristic algorithms presented in the literature do not fit with the objective function (Gnetchejo *et al.*, 2019). The *RMSE* values are not calculated correctly since the estimated PV output

current is incorrect (Ćalasan *et al.*, 2019). In order to be careful about the accuracy, the results should be cross-checked.

This study aimed to propose a triangular adaptive differential evolution (TADE) algorithm to estimate parameters from PV cells and modules and evaluate their *I–V* and *P-V* characteristics.

2. MATERIALS AND METHODS:

Four case studies were carried out to assess the performance of the TADE algorithm. In the first and second cases, SDM and DDM were implemented to estimate the RTC-France PV cell parameters under irradiance and temperature about 1000 W/m^2 and 33˚C, respectively. The experimental data consisted of 26 pairs of voltage and current values extracted from the experimental data in (Ma., 2014). In the third case, PMM was applied to estimate the Photowatt-PWP201 PV module parameters, which had 36 series-connected polycrystalline silicon cells under the irradiance and temperature of about 1000 W/m^2 and 45˚C, respectively. The experimental data contained 25 pairs of voltage-current values were obtained from (Ma., 2014). The last case referred to the KC200GT PV module, which consisted of 54 series connected polycrystalline silicon cells. The experimental data of the KC200GT PV module were obtained under varied environmental measurements.

2.1. Photovoltaic Model and Problem Formulation

In this section, the single-diode model (SDM), the double-diode model (DDM), the photovoltaic module model (PMM), and the problem formulation were represented. The PV cells and modules equivalent circuits can be described by using a current source with diodes connected in series or parallel, one resistor connected in series, and the other resistor connected in parallel.

2.1.1 Single-Diode Model

The electrical equivalent circuit of SDM for PV cells is illustrated in Figure 1. The SDM consists of a current source, diode, series resistance, and shunt resistance. The current source (I_{PV}) is a photogenerated current. The current flowing through the diode (I_D) is the diffusion current produced by the majority carrier (Hejri *et al.*, 2014). The series resistance (R_S) is the internal resistance that causes voltage drops and power losses when current is flowing, while the shunt resistance (R_P) is the resistance due to leakage current in the junction of p-n PV cells. The diffusion current can be calculated as follows:

$$I_D = I_O \left\{ \exp\left[\frac{(V+IR_S)}{AV_{TH}} \right] - 1 \right\} \quad \text{(Eq. 1)}$$

According to the equivalent circuit in Figure 1, the output current and power of the PV cell in SDM are expressed as follows (Wolf *et al.*, 1977):

$$I = I_{PV} - I_O \left\{ \exp\left[\frac{(V+IR_S)}{AV_{TH}} \right] - 1 \right\} - \frac{V+IR_S}{R_P} \quad \text{(Eq. 2)}$$

$$P = \left\{ I_{PV} - I_O \left\{ \exp\left[\frac{(V+IR_S)}{AV_{TH}} \right] - 1 \right\} - \frac{V+IR_S}{R_P} \right\} V \quad \text{(Eq. 3)}$$

In Equations (2) and (3), I_{PV} is the photogenerated current, I_O is the reverse saturation current, A is the ideality factor, V is the PV output voltage, I is the PV output current, and V_{TH} is the thermal voltage. The thermal voltage is depicted by

$$V_{TH} = N_S kT/q \quad \text{(Eq. 4)}$$

where N_S is the number of PV cells connected in series, k is the Boltzmann constant (k = 1.38E-23 J/K), q is the electron charge (q = 1.6E-19 C), and T is the absolute temperature of the PV cell measured in Kelvin.

In the SDM, the five parameters, i.e., I_{PV}, I_O, R_S, R_P, and A, are considered as unknown parameters to be estimated.

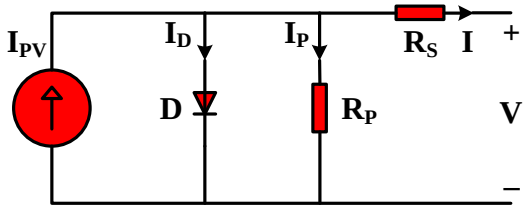

Figure 1. *The equivalent circuit for the single-diode model*

2.1.2 Double-Diode Model

Unlike the SDM, the DDM has two diodes in the equivalent circuit, as shown in Figure 2. In the DDM, the recombination current is taken into account (Fuchs and Sigmund, 1986). The diffusion current due to majority carrier (I_{D1}) and the recombination current due to minority carrier (I_{D2}) can be calculated as follows:

$$I_{D1} = I_{O1} \left\{ \exp\left[\frac{(V+IR_S)}{A_1 V_{TH}} \right] - 1 \right\} \quad \text{(Eq. 5)}$$

$$I_{D2} = I_{O2}\left\{\exp\left[\frac{(V+IR_S)}{A_2V_{TH}}\right] - 1\right\} \quad \text{(Eq. 6)}$$

In Equations (4) and (5), I_{O1} and I_{O2} are respectively reverse saturation currents due to the diffusion and the recombination phenomenon. The diffusion and recombination ideality factors are denoted by A_1 and A_2, respectively. Thus, the output current is as follows:

$$I = I_{PV} - I_{O1}\left\{\exp\left[\frac{(V+IR_S)}{A_1V_{TH}}\right] - 1\right\} - I_{O2}\left\{\exp\left[\frac{(V+IR_S)}{A_2V_{TH}}\right] - 1\right\} - \frac{V+IR_S}{R_P} \quad \text{(Eq. 7)}$$

The power generated by the PV cell is

$$P = \left\{I_{PV} - I_{O1}\left\{\exp\left[\frac{(V+IR_S)}{A_1V_{TH}}\right] - 1\right\} - I_{O2}\left\{\exp\left[\frac{(V+IR_S)}{A_2V_{TH}}\right] - 1\right\} - \frac{V+IR_S}{R_P}\right\}V \quad \text{(Eq. 8)}$$

Hence, for the DDM, seven unknown parameters must be estimated, i.e., I_{PV}, I_{O1}, I_{O2}, R_S, R_P, A_1, and A_2.

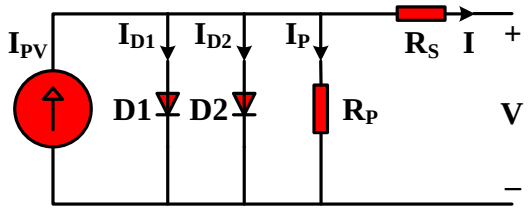

Figure 2. *The equivalent circuit for the double-diode model*

2.1.3 Photovoltaic Module Model

A PV module is constructed by a sufficient number of PV cells, which are connected in series and parallel to increase the level of output power. Figure 3 presents the equivalent circuit of a PV module. The output current for the PMM is expressed as:

$$I = N_PI_{PV} - N_PI_O\left\{\exp\left[\frac{(V+IR_S(N_S/N_P))}{AV_{TH}N_S}\right] - 1\right\} - \frac{V+IR_S(N_S/N_P)}{R_P(N_S/N_P)} \quad \text{(Eq. 9)}$$

The power output of the PV module is

$$P = \left\{N_PI_{PV} - N_PI_O\left\{\exp\left[\frac{(V+IR_S(N_S/N_P))}{AV_{TH}N_S}\right] - 1\right\} - \frac{V+IR_S(N_S/N_P)}{R_P(N_S/N_P)}\right\}V \quad \text{(Eq. 10)}$$

where N_P denotes the number of PV cells in parallel and N_S is the number of PV cells in series.

For simplicity, Equations. (9) and (10) can be rewritten as

$$I = I_{PVM} - I_{OM}\left\{\exp\left[\frac{(V+IR_{SM})}{A_MV_{TH}}\right] - 1\right\} - \frac{V+IR_{SM}}{R_{PM}} \quad \text{(Eq. 11)}$$

$$P = \left\{I_{PVM} - I_{OM}\left\{\exp\left[\frac{(V+IR_{SM})}{A_MV_{TH}}\right] - 1\right\} - \frac{V+IR_{SM}}{R_{PM}}\right\}V \quad \text{(Eq. 12)}$$

where $I_{PVM} = N_PI_{PV}$, $I_{OM} = N_PI_O$, $R_{SM} = (N_S/N_P)R_S$, $R_{PM} = (N_S/N_P)R_P$, $A_M = N_SA$.

Considering the PMM, five unknown parameters, i.e., I_{PVM}, I_{OM}, R_{SM}, R_{PM}, and A_M, are estimated according to the *I-V* data of real PV modules.

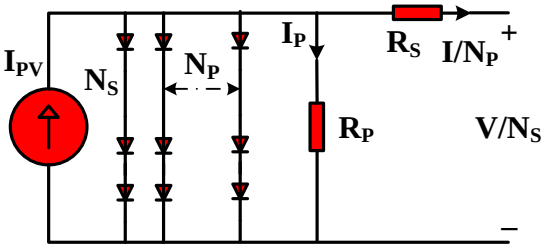

Figure 3. *The equivalent circuit for the photovoltaic module model*

2.1.4 Problem Formulation

The parameters of PV cells and modules are unknown and variable with temperature and solar irradiance (Chaibi *et al.*, 2019). Thus, the estimation of PV parameters can be represented as an optimization problem, aiming to minimize the difference between the measured and the estimated I-V data. The problem here is defined as an objective function used for the optimization process.

In this study, the *RMSE* method is applied to describe objective functions. The *RMSE* method compares the difference between the measured and the estimated values. The *RMSE* for the photovoltaic problem is expressed as

$$RMSE = \sqrt{\frac{1}{N}\sum_{j=1}^{N}\left[f_j(V,I,\emptyset)\right]^2} \quad \text{(Eq. 13)}$$

$$f_j(V,I,\emptyset) = I_j - I_{estj} \quad \text{(Eq. 14)}$$

where N is the number of measured *I-V* data points, V and I are the measured voltage and current, respectively, and $\emptyset$ is a vector containing the parameters to be calculated.

The difference between the measured

current (I) and the estimated current (I_{est}) at a point of the I-V curve is an individual error (IE), which is defined by the error function (f (V, I, ∅)).

The estimated current of the SDM is then formulated as

$$I_{est} = I_{PV} - I_O \left\{ \exp\left[\frac{(V+IR_s)}{AV_{TH}}\right] - 1 \right\} - \frac{V+IR_s}{R_p} \quad \text{(Eq. 15)}$$

For the DDM, the estimated current is

$$I_{est} = I_{PV} - I_{O1} \left\{ \exp\left[\frac{(V+IR_s)}{A_1 V_{TH}}\right] - 1 \right\} - I_{O2} \left\{ \exp\left[\frac{(V+IR_s)}{A_2 V_{TH}}\right] - 1 \right\} - \frac{V+IR_s}{R_p} \quad \text{(Eq. 16)}$$

and the estimated current for the PMM is defined as

$$I_{est} = I_{PVM} - I_{\mathrm{OM}} \left\{ \exp\left[\frac{(V+IR_{SM})}{A_M V_{TH}}\right] - 1 \right\} - \frac{V+IR_{SM}}{R_{PM}} \quad \text{(Eq. 17)}$$

The error functions of the SDM, DDM, and PMM are summarized in Table 1.

2.2. Triangular Adaptive Differential Evolution Algorithm

Differential evolution (DE) is a population-based stochastic optimization algorithm. The advantages of the DE are (Ridha *et al.*, 2020): a) it can increase the search space capacity, b) it can find the optimal minimum from a multi-model search, and c) it has a robust mutation scheme. This evolution algorithm utilizes two control parameters, i.e., the mutation factor (F) and the crossover rate (CR). These two parameters control perturbance and enhance the convergence speed of the computation process. The triangular adaptive differential evolution (TADE) algorithm employs a triangular probability distribution and a population reduction strategy to improve the convergence speed during the evolution process

2.2.1 Initialization and Evaluation

The first step in the DE optimization process is initialized by randomly generating an initial population as the candidate solutions within defined boundaries. Such candidates must lie inside the feasible lower and upper bounds. If the population size is NP and the dimension of the problem is D, the initialization is assigned by

$$x_{i,j}^{(G=1)} = x_{minj} + rand_j\left(x_{maxj} - x_{minj}\right) \quad \text{(Eq. 18)}$$

where $x_{i,j}^{(G=1)}$ is the initial population at generation-1, x_{minj} and x_{maxj} are the lower and upper bounds of the individuals, and $rand_j \in [0, 1]$, $j = 1, 2, \ldots, D$; $i = 1, 2, \ldots, NP$.

Evaluation of the population is employed to find which individuals of the current population will be the best candidates to satisfy the fitness value. The best individuals are selected by using

$$f_{bestj}^{(G)} = f\left(x_{bestj}^{(G)}\right), x_{bestj}^{(G)} \in x_{i,j}^{(G)} \quad \text{(Eq. 19)}$$

2.2.2 Parameter Adaptation

The control parameters at generation G, i.e., $F_i^{(G)}$ and $CR_i^{(G)}$, are adapted by applying triangular probability distribution as follows:

if $rand_j < \tau$

$$\alpha_i^{(G)} = \alpha_{min} + \left[rand_j(\alpha_{max} - \alpha_{min})(\alpha_{mod} - \alpha_{min})\right]^{0.5} \quad \text{(Eq. 20)}$$

otherwise,

$$\alpha_i^{(G)} = \alpha_{max} - \left[\left(1 - rand_j\right)(\alpha_{max} - \alpha_{min})(\alpha_{max} - \alpha_{mod})\right]^{0.5} \quad \text{(Eq. 21)}$$

where,

$$\tau = (\alpha_{mod} - \alpha_{min})/(\alpha_{max} - \alpha_{min}) \quad \text{(Eq. 22)}$$

The probability distribution within [0,1] is determined by using three values, i.e., the lower limit (α_{min}), the mode (α_{mod}), and the upper limit (α_{max}). In this case, $\alpha_{min} \le \alpha_{mod} \le \alpha_{max}$.

2.2.3 Mutation, Crossover, and Selection

The mutation operation creates mutant individuals $v_{i,j}^{(G)}$ by perturbing randomly selected individuals with the difference between the two other randomly selected individuals. The TADE algorithm adopts the "DE/rand/2" mutation strategy, which is defined as:

$$v_{i,j}^{(G)} = x_{r1,j}^{(G)} + F_i^{(G)}\left(x_{r2,j}^{(G)} - x_{r3,j}^{(G)}\right) + F_i^{(G)}\left(x_{r4,j}^{(G)} - x_{r5,j}^{(G)}\right) \quad \text{(Eq. 23)}$$

In the mutation process, the indices $r1$, $r2$, $r3$, $r4$, and $r5$ are taken randomly from [1, NP]. The integers i, $r1$, $r2$, $r3$, $r4$, and $r5$, are randomly chosen mutually exclusive integers and must be different from each other and also different from

the base index *i*.

The crossover operation increases the diversity of the mutant individual by generating trial individuals $t_{i,j}^{(G)}$. TADE employs a binomial crossover strategy, which is expressed as:

$$t_{i,j}^{(G)} = \begin{cases} v_{i,j}^{(G)}, if\ \left(rand_j \le CR_i^{(G)}\right) or (j = j_{rand}) \\ x_{i,j}^{(G)}, otherwise \end{cases} \quad \text{(Eq. 24)}$$

where i = 1,2,…,NP, j = 1,2,…,D, and j_{rand} is a randomly chosen number $\in$ {1,2,…,D} that guarantees $t_{i,j}^{(G)}$ to get at least one parameter from $v_{i,j}^{(G)}$.

Finally, the selection process compares the fitness values of the parents and trial individuals. The trial individuals are accepted for the next generation if and only if they have equal or lower fitness value than their parents. The selection operation is represented as:

$$x_{i,j}^{(G+1)} = \begin{cases} t_{i,j}^{(G)}, if\ f\left(t_{i,j}^{(G)}\right) \le f\left(x_{i,j}^{(G)}\right) \\ x_{i,j}^{(G)}, otherwise \end{cases} \quad \text{(Eq. 25)}$$

The best individuals are also selected here as

$$f_{bestj}^{(G+1)} = f\left(x_{bestj}^{(G+1)}\right), x_{bestj}^{(G+1)} \in x_{i,j}^{(G+1)} \quad \text{(Eq. 26)}$$

2.2.4 Population Size Reduction Strategy

In the DE algorithm, the population size *NP* is constant throughout the evolution process. In order to enhance the convergence rate of the TADE algorithm, a population size reduction strategy is applied to improve the exploitation and exploration processes. The population size reduction strategy is dynamically resizing the population during the evolution process [63]. After each generation *G*, the next-generation population size, $NP^{(G+1)}$, is computed according to the formula:

$$NP^{(G+1)} = round\left[\left(\frac{NP_{min} - NP^{(G)}}{MNFE}\right) NFE + NP^{(G)}\right] \quad \text{(Eq. 27)}$$

where $NP^{(G=1)}$ is the population size at generation 1 is, NP_{min} is the population size at the end evolution process, *NFE* is the number of fitness evaluations, and *MNFE* is the maximum *NFE*. The value of NP_{min} is set to the smallest possible value such that the evolutionary operator is usable. In the case of TADE, NP_{min} is set to 5 due to the "DE/rand/2" mutation strategy in this study requires five individuals. Whenever $NP^{(G+1)} < NP^{(G)}$, the ($NP^{(G)} - NP^{(G+1)}$) individuals with worse fitness values are eliminated from the population. The steps involved in the TADE algorithm are tabulated in Algorithm 1.

3. RESULTS AND DISCUSSION:

3.1. Estimation of the Parameters of the RTC-France PV Cell

The SDM has five parameters to be determined. The typical design space of photogenerated current (I_{PV}), reverse saturation current (I_O), ideality factor (A), series resistance (R_S), and shunt resistance (R_P), are chosen to be within the range {0, 1} A, {0, 1} μA, {1, 2}, {0, 0.5} Ω, and {0, 100} Ω, respectively.

For the SDM, the performance results of TADE are compared with those of TLABC (Chen *et al.*, 2018a), IJAYA (Yu *et al.*, 2017a), GWOCS (Long *et al.*, 2020), SATLBO (Yu *et al.*, 2017b), DE, and TADE. The experimental results are obtained after 30 independent runs. Table 2 represents the estimated parameters of six distinct algorithms with their best, worst, mean, and standard deviation values of *RMSE*, respectively. Additionally, the *MNFE* of the convergence processes is also shown in the last row of Table 2. It should be noted that the lower the *RMSE* value, the more precise the estimation results of these PV parameters will be. Moreover, the low standard deviation indicates high reliability, while the mean value of *RMSE* quantifies the average accuracy of the algorithm.

From the results in Table 2, according to their best values of *RMSE*, all SATLBO, TLABC, DE, and TADE achieve the best result (i.e., 9.8602×10^{-04}), followed by GWOCS (i.e., 9.8607×10^{-04}) and IJAYA (i.e., 9.8603×10^{-04}). Both IJAYA and GWOCS obtain slightly higher best values of RMSE. Considering the standard deviation, mean, and worst of *RMSE*, TADE outperforms the other five algorithms. It is also observed that DE and TADE need less *MNFE* compared to different algorithms.

The convergence of the six compared algorithms for the SDM is presented in Figure 4. This figure clearly shows that TADE gives the fastest convergence performance, subsequently DE, GWOCS, IJAYA, TLABC, and SATBLO. The TADE and DE algorithms require less than 10000 and 20000 NFEs to reach their best *RMSE*, respectively. Figure 4 also shows that GWOCS,

TLABC, SATLBO, and IJAYA converge after 20000 number of function evaluations. Both GWOCS and IJAYA perform faster convergence than TLABC and SATLBO. But on the other hand, TLABC and SATLBO can find more accurate *RMSE* values than GWOCS and IJAYA.

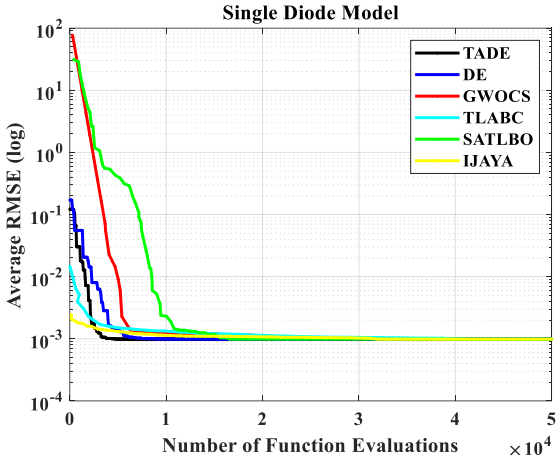

Figure 4. *Convergence processes of the six algorithms for the RTC-France PV cell (SDM)*

Further investigations were carried out to assess the quality of estimated parameters and avoid inaccuracies in the TADE results. The estimated parameter values of the SDM, i.e., I_{PV}, I_O, A, R_S, and R_P, are entered into Equation (13). For TADE, the values of parameters found are I_{PV} = 0.76077553 A, I_O = 0.32302083x10^{-06} A, R_S = 0.03637709 Ω, R_P = 53.71852506 Ω, and A = 1.48118360. The *RMSE* result is 9.860219x10^{-04}, and this matches correctly.

Table 3 lists the *RMSE* value obtained by the TADE compared with other algorithms. It is seen that the *RMSE* value of the TADE algorithm is 9.860219x10^{-04}, and this value is as small as most of the algorithms, but in the different significant digits. However, the *RMSE* of the TADE algorithm is smaller than the *RMSE* values of SOS, MSSO, MABC, BLPSO, and GOTLBO. It is also seen that the BLPSO algorithm has the worst result, which the *RMSE* is 11.239x10^{-04}.

The individual abs(error) (*IAE*) and *I-V* and *P-V* curves between the measured and the estimated data over the entire voltage range are presented in Table 4 and Figure 5. Table 4 exhibits the measured and estimated currents and powers for the RTC-France PV cell at 26 different working conditions. The individual abs(error) values describe the error between the measured and the calculated data. The small *IAE* indicates the excellent estimated data. As seen in Table 4 and Figure 5(b), the values of individual abs(error) of current are less than 0.003 Ampere, while the values of individual abs(error) of power are less than 0.002 Watt. With these low errors, the measured data gained by TADE fits perfectly into the estimated data of the RTC-France PV cell, as shown in Figure 5(a). Table 4 and Figure 5 show that the PV parameters estimated by TADE have pretty good accuracy.

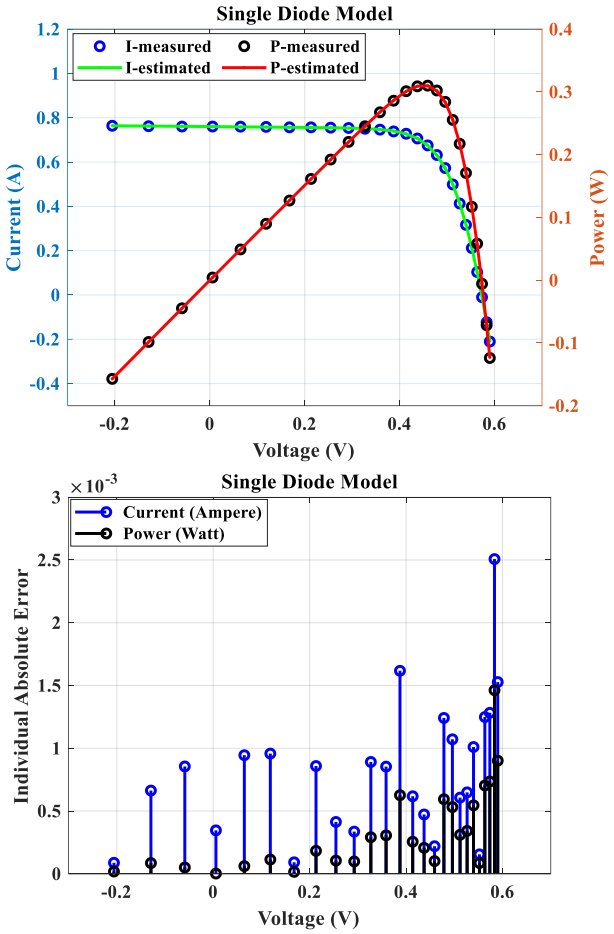

Figure 5. E*stimated and measured data of SDM: (a) I-V/P-V curves, (b) Individual abs(error)*

In the second case, the parameter estimation of the RTC-France PV cell was carried out by using DDM. The DDM has seven parameters to optimize. Increasing the number of parameters will increase the difficulty level of the parameter estimating process. In this case, the typical design space of I_{PV}, I_{o1}, I_{o2}, A_1, A_2, R_S, and R_P, are specified within the range {0, 1} A, {0, 1} μA, {0, 1} μA, {1, 2}, {1, 2}, {0, 0.5} Ω, and {0, 100} Ω, respectively. Table 5 shows the estimated parameters and the *RMSE* values. The results acquired by TLABC, IJAYA, GWOCS, SATLBO, DE, and TADE are considered for comparison. Similar to the previous case, the results in Table 5 are obtained after 30 independent runs.

It is seen from Table 5 that the best value of *RMSE* obtained by TADE is as low as

9.8243x10^{-04}. The TADE algorithm also performs the best result in terms of the mean, standard deviation, and worst *RMSE*. It verifies that TADE is the most accurate among the algorithms being compared. It is also observed in Table 5 that both DE and TADE require less *MNFE* compared to other algorithms. Tables 2 and 5 show that TADE gives the best precision and reliability on both SDM and DDM on account it outperforms the five different algorithms regarding the best, worst, mean, and standard deviation of the *RMSE*. It is further observed that, as expected, the best *RMSE* values obtained in the DDM case are smaller than the value obtained for the SDM case. It is noted that DDM should estimate the unknown PV parameters more accurately than SDM.

To verify the convergence speed of the TADE algorithm, Figure 6 exhibits the convergence processes of six algorithms. The TADE performs the fastest convergence speed, and then subsequently DE, TLABC, IJAYA, GWOCS, and SATLBO. The TADE needs less than 20000 function evaluations to reach the best *RMSE*, which is the fastest convergence process of all the algorithms, as shown in Table 5 and Figure 6. Other algorithms converge after 20000 NFEs. Figure 6 also demonstrated that DE and TLABC converge much faster than GWOCS and SATLBO. Although it has the slowest convergence speed of all, SATLBO can achieve the best *RMSE* accuracy, which is better than other algorithms, except TADE.

The PV parameters found must fit the *RMSE*. In order to avoid inaccuracies occurred in the results, the estimated parameters can be cross-checked by using Equation (13). The parameters are I_{PV} = 0.76077887 A, I_{O1} = 0.57982851x10^{-06} A, I_{O2} = 0.26238944x10^{-06} A, R_S = 0.03661196 Ω, R_P = 54.88852821 Ω, A_1 = 2.06856333, and A_2 = 1.46322217. The *RMSE* result is 9.824321x10^{-04}. This value matches the *RMSE* value found by the TADE algorithm very well.

A deeper investigation of the DDM of RTC-France PV cell found that the *RMSE* value can be as small as 9.727248x10^{-04} if the search range of A_1 is within {1, 3}. It is observed that the corresponding parameters with the *RMSE* of 9.727248x10^{-04} are: I_{PV} = 0.760777759 A, I_{O1} = 6.92409709x10^{-06} A, I_{O2} = 0.260629884x10^{-06} A, R_S = 0.036751455 Ω, R_P = 57.63085158 Ω, A_1 = 2.931617412, and A_2 = 1.461203635. It is noted that for this *RMSE* value, A_1 = 2.931617412 is in the search range of {1, 3}. The estimated *RMSE* values of the DDM for TADE and other recent algorithms from literature are also summarized in Table 6. It is seen that TADE gives the *RMSE* value of 9.824321x10^{-04}, and this is the most accurate *RMSE* value among all compared algorithms. These results prove that TADE yields the highest accuracy in estimating the PV parameters of the DDM. By comparing Tables 3 and 6, as expected, it is also observed that TADE performance for DDM is better than for SDM.

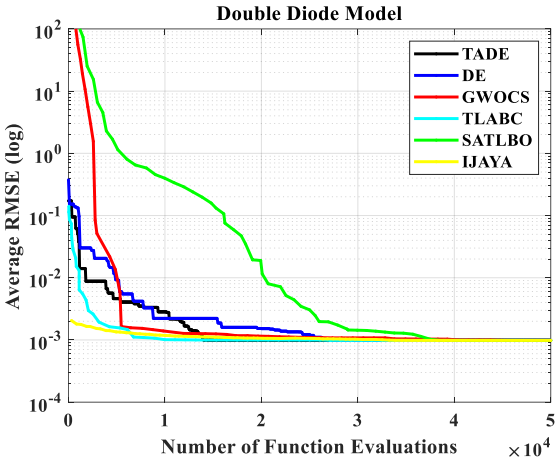

Figure 6. *Convergence processes of the six algorithms for the RTC-France PV cell (DDM)*

Table 7 and Figure 7 show the individual abs(error) values and the *I-V* / *P-V* curves obtained by the TADE algorithm. Table 6 represents the measured and estimated currents and powers for the RTC-France PV cell at 26 different working conditions. As shown in Table 7 and Figure 7(b), the individual abs(error) values are less than 0.003 and 0.02 for current and power, respectively.

It indicates that the estimated data are reasonably very close to the measured data, meaning that TADE has an excellent capability in estimating parameters of DDM. The measured and calculated data are in perfect agreement, as shown in Figure 7(a). These confirm the high accuracy of the TADE algorithm for the PV parameter estimation of DDM.

3.2. Estimation of the Parameters of the Photowatt-PWP-201 PV Module

The PMM has five parameters to be determined. The typical range of I_{PVM}, I_{OM}, A_M, R_{SM}, and R_{PM} for Photowatt-PWP 201 PV module are defined by {0, 2} A, {0, 50} μA, {1, 50}, {0, 2} Ω, and {0, 2000} Ω, respectively. Similar to the previous cases, estimating the Photowatt-PWP 201 PV module parameters is carried out by using six compared algorithms, i.e., TLABC, IJAYA, GWOCS, SATLBO, DE, and TADE. The results are obtained after 30 independent runs and tabulated in Table 8.

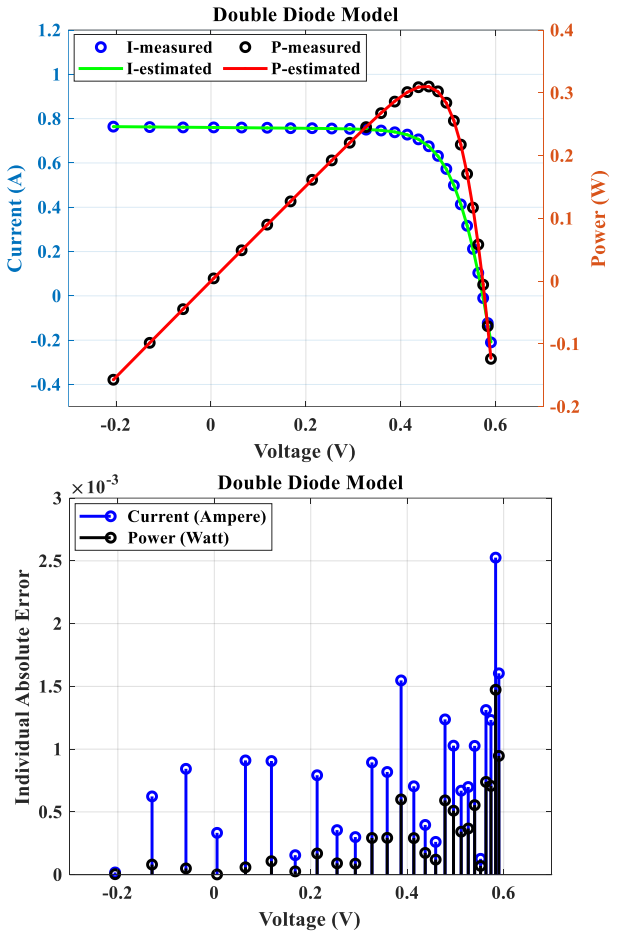

Figure 7. *Estimated and measured data of DDM: (a) I-V/P-V curves, (b) Individual abs(error)*

It is seen from Table 8 that all six algorithms, including IJAYA, SATLBO, TLABC, GWOCS, DE, and TADE, obtain the smallest best value of *RMSE*, which is as low as 2.4251x10^{-03}. In terms of the standard deviation, TADE has the best result. Table 8 also shows that TADE obtains the smallest mean and worst values of *RMSE*. Moreover, TADE also requires less *MNFE* compared to IJAYA, SATBLO, TLABC, and GWOCS. Consequently, these prove that TADE can achieve highly accurate and reliable PV parameters on PMM because it outperforms the other five algorithms regarding the best, worst, mean, and *SD* values of *RMSE*. Furthermore, the *RMSE* value is plotted versus the number of function evaluations. In terms of the convergence speed, TADE yields the best performance for estimating the Photowatt-PWP 201 PV module parameters, as shown in Figure 8. All six algorithms achieve the same best *RMSE* values, but TADE performs the fastest convergence, subsequently DE, GWOCS, TLABC, IJAYA, and SATBLO. The simulations show that TADE requires less than 10000 NFEs to meet the best *RMSE* value. This result proves that the TADE algorithm has a speedy convergence performance.

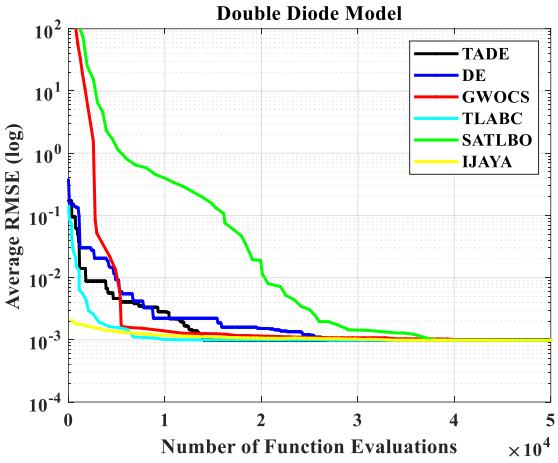

Figure 8. *Convergence curves of the six algorithms for Photowatt PWP-201 PV module (PMM)*

To avoid inaccuracies in the results, the *RMSE* should be cross-checked using estimated values of I_{PVM}, I_{OM}, A_M, $R_{SM,}$ and R_{PM}, and measured current and voltage data. For TADE, the values of parameters found are I_{PVM} = 1.03051430 A, I_{OM} = 3.48226301x10^{-06} A, R_{SM} = 1.20127101 Ω, R_{PM} = 981.98228397 Ω, and A_M = 48.64283497. The *RMSE* result is 2.425075x10^{-03} and this value matches correctly. Additionally, the estimated values of *RMSE* obtained by TADE and other recent algorithms from literature are listed in Table 9. Like the SDM case, Table 9 shows that TADE, together with most of the algorithms, acquire the same *RMSE* values in the different significant digits, except the TVACPSO algorithm, which yields the worst *RMSE* value.

Furthermore, Table 10 and Figure 9 are used to confirm the accuracy of TADE. Table 10 shows the measured and estimated currents and powers for the Photowatt PWP-201 PV module at 25 different working conditions. As seen in Table 10 and Figure 9, the individual abs(error), and the measured and estimated *I-V*/*P-V* curves show that they have a remarkable coincidence throughout the entire voltage range. Table 10 and Figure 9(b) show that the values of individual abs(error) of current are less than 0.005 Ampere, while the values of individual abs(error) of power are less than 0.08 Watt. These *IAE* values are small enough for a PV module and demonstrate the accuracy of estimated accuracy. Figure 9(a) shows a good matching between the measured and calculated data with these tiny errors. This observation, once more, verifies the accuracy of the TADE algorithm.

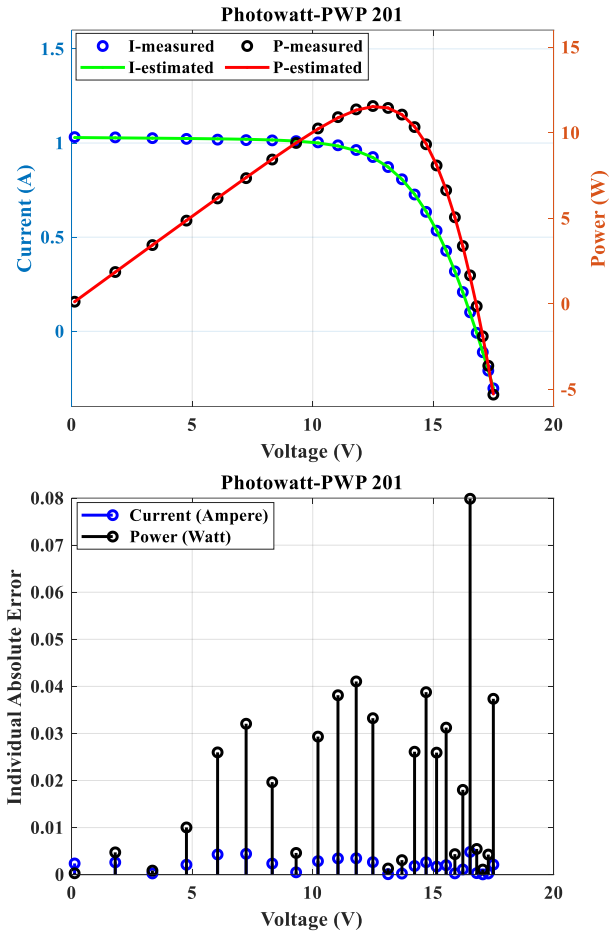

Figure 9. *Estimated and measured data of the Photowatt-PWP-201 PV module: (a) I-V/P-V curves, (b) Individual abs(error)*

Additionally, the Friedman test (Alcalá-Fdez *et al.*, 2009) on SDM, DDM, and PMM PV parameter estimation problems is conducted to show the performance ranking of six algorithms. The results demonstrate that TADE achieves the best average ranking (1.40), followed by DE (2.67), GWOCS (4.63), IJAYA (5.76), TLABC (6.21), and SATLBO (7.93), as shown in Figure 10. According to the comparison results, it is evident that TADE has a high competitive achievement in the accuracy, reliability, and convergence speed of PV parameter estimation against the other algorithms.

3.3. Estimation of the Parameters of the KC200GT PV Module

In this section, the TADE algorithm is evaluated using a KC200GT PV module operating under various weather conditions. The KC200GT PV module experimental data at five solar irradiations and three different temperatures are used to investigate the influence of the irradiance and temperature on the performance of the TADE algorithm. These observations are important to estimate PV parameters under partial shading or different weather conditions (Chen *et al.*, 2019a). The typical design range of I_{PVM}, I_{OM}, A_M, R_{SM}, and R_{PM} for KC200GT PV module are chosen to be {0, 10} A, {0, 3} μA, {1, 500}, {0, 100} Ω, and {0, 1} Ω, respectively.

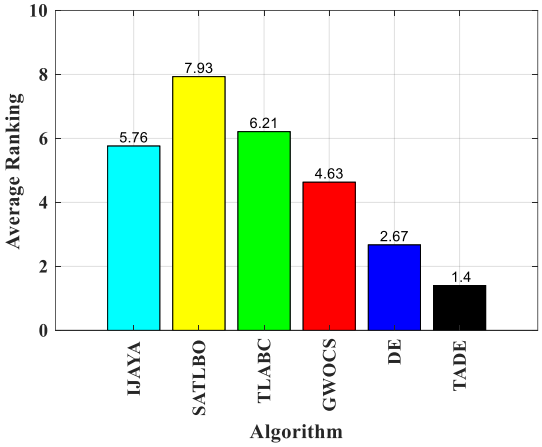

Figure 10. *Friedman test results*

Table 11 presents the PV parameters estimation for the KC200GT PV module at various solar irradiation and temperature levels. Table 11 shows that under different solar irradiation levels and a constant temperature of 25℃, the TADE algorithm can estimate PV parameters with acceptable values of *RMSE*. Similarly, the TADE algorithm also works very well in acquiring the PV parameters under a constant irradiance of 1000 W/m^2 and various temperature conditions. From Table 11, it can also be seen that I_{PVM} is increased while I_{OM}, R_{SM}, R_{PM}, and A_M are decreased as the irradiance increasing. On the other hand, it can be found that I_{PVM} is increased while I_{OM}, R_{SM}, R_{PM}, and A_M are fluctuation as the temperature increases.

Again, to find out the accuracy of estimated parameters, the *I-V* and *P-V* curves of the KC200GT PV module at various irradiation and temperature conditions are plotted, as shown in Figures 11 and 12. It can be observed that under different irradiation and temperature conditions, the estimated and measured *I-V* and *P-V* curves are near enough. These results indicate that the TADE algorithm also performs well in estimating the PV module parameters under various irradiances and temperatures.

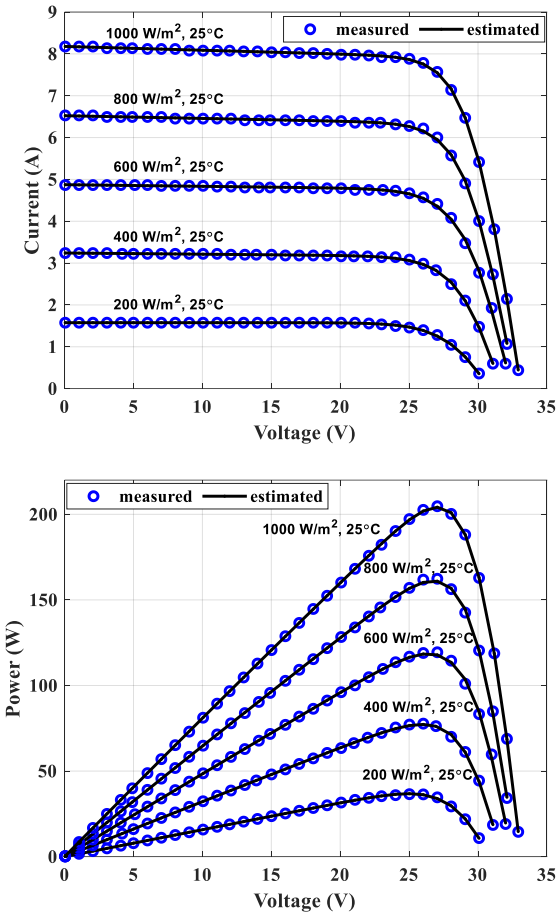

Figure 11. *Estimated and measured data of TADE for the KC200GT PV module under various irradiances*

4. CONCLUSIONS:

TADE algorithm was successfully applied for optimally estimating the PV cell and module parameters. The experimental and statistical results showed that the TADE was outperformed most of the algorithms in accuracy, reliability, and convergence speed. Moreover, estimating PV parameters at different irradiance and temperature conditions also proved that the TADE algorithm could get outstanding results. Therefore, the proposed TADE algorithm could be recommended as an accurate and reliable technique for estimating PV cell and module parameters.

5. ACKNOWLEDGMENTS:

This study is conducted with financial support from DIPA Fakultas Teknik UNTAN 2021.

6. REFERENCES:

1. Abbassi, R; Abbassi, A; Heidari, A. A; Mirjalili, S. (2019). An efficient salp swarm-inspired algorithm for parameters identification of photovoltaic cell models. *Energy Conversion and Management*, 179, 362-372.

2. Alcalá-Fdez, J; Sánchez, L; Garcia, S; del Jesus, M. J; Ventura, S; Garrell, J. M; Otero, J; Romero, C; Bacardit, J; Rivas, V. M; Fernández, J. C; Herrera, F. (2009). KEEL: a software tool to assess evolutionary algorithms for data mining problems. *Soft Computing*, 13, 307-318.

3. Anani, N; Ibrahim, H. (2020). Adjusting the single-diode model parameters of a photovoltaic module with irradiance and temperature. *Energies*, 13(12), 3226.

4. Arabshahi, M. R; Torkaman, H; Keyhani, A. (2020). A method for hybrid extraction of single-diode model parameters of photovoltaics. *Renewable Energy*, 158, 236-252.

5. Beigi, A. M; Maroosi, A. (2018). Parameter identification for solar cells and module using a Hybrid Firefly and Pattern Search Algorithms. *Solar Energy*. 171, 435-446.

6. Bosman, L. B; Leon-Salas, W. D; Hutzel, W; Soto, E. A. (2020). PV system predictive maintenance: challenges, current approaches, and opportunities. *Energies*, 13(6), 1398.

7. Ćalasan, M; Jovanović, D; Rubežić, V; Mujović, S; Đukanović, S. (2019). Estimation of single-diode and two-diode solar cell parameters by using a chaotic optimization approach. *Energies*, 12(21), 4209.

8. Ćalasan, M; Aleem, S. H. E. A; Zobaa, A. F. (2020). On the root mean square error (RMSE) calculation for parameter estimation of photovoltaic models: A novel exact analytical solution based on Lambert W function. *Energy Conversion and Management*, 210, 112716.

9. Chaibi, Y; Allouhi, A; Malvoni, M; Salhi, M; Saadani, R. (2019). Solar irradiance and temperature influence on the photovoltaic cell equivalent-circuit models. *Solar Energy*, 188, 1102-1110.

10. Chen, X; Tianfield, H; Mei, C; Du, W; Liu,

G. (2017). Biogeography-based learning particle swarm optimization. *Soft Computing*, 21, 7519-7541.

11. Chen, Y; Sun, Y; Meng, Z. (2018a). An improved explicit double-diode model of solar cells: Fitness verification and parameter extraction. *Energy Conversion and Management*, 169, 345-358.

12. Chen, X; Xu, B; Mei, C; Ding, Y; Li, K. (2018b) Teaching learning-based artificial bee colony for solar photovoltaic parameter estimation. *Applied Energy*, 212, 1578-1588.

13. Chen, X; Yue, H; Yu, K. (2019a). Perturbed stochastic fractal search for solar PV parameter estimation. *Energy*, 189, 116247.

14. Chen, H; Jiao, S; Heidari, A. A; Wang, M; Chen, X; Zhao, X. (2019b). An opposition-based sine cosine approach with local search for parameter estimation of photovoltaic models. *Energy Conversion and Management*, 195, 927-942.

15. Chen, X; Yu, K. (2019c). Hybridizing cuckoo search algorithm with biogeography-based optimization for estimating photovoltaic model parameters. *Solar Energy*, 180, 192-206.

16. El-Naggar, K. M; AlRashidi, M. R; AlHajri, M. F; Al-Othman; A. K. (2012). Simulated Annealing algorithm for photovoltaic parameters identification. *Solar Energy Conversion and Management*, 86(1), 266-274.

17. Et-torabi, K; Nassar-eddine, I; Obbadi, A; Errami, Y; Rmaily, R; Sahnoun, S; El Fajri, A; Agunaou, M. (2017). Parameters estimation of the single and double diode photovoltaic models using a Gauss-Seidel algorithm and analytical method: A comparative study. *Energy Conversion Management*, 148, 1041-1054.

18. Fuchs; D; Sigmund, H. (1986). Analysis of the current-voltage characteristic of solar cells. *Solid-State Electronics*, 29(8), 791-795.

19. Gao, X; Cui, Y; Hu, J; Xu, G; Yu, Y. (2016). Lambert W-function based exact representation for double diode model of solar cells: Comparison on fitness and parameter extraction. *Energy Conversion and Management*, 127, 443-460.

20. Gao, X; Cui, Y; Hu, J; Xu, G; Wang, Z; Qu, J; Wang, H. (2018). Parameter extraction of solar cell models using improved shuffled complex evolution algorithm. *Energy Conversion and Management,* 157, 460-479.

21. Ghani, F; Rosengarten, G; Duke, M; Carson, J. K. (2014). The numerical calculation of single-diode solar-cell modelling parameters. *Renewable Energy*, 72, 105-112.

22. Gnetchejo, P. J; Essiane, S. N; Ele, P; Wamkeue, R; Wapet, D. M; Ngoffe, S. P. (2019). Important notes on parameter estimation of solar photovoltaic cell. *Energy Conversion and Management*, 197, 111870.

23. Hejri, M; Mokhtari, H; Azizian, M. R; Ghandhari, M; Soder, L. (2014). On the parameter extraction of a five-parameter double-diode model of photovoltaic cells and modules. *IEEE Journal of Photovoltaic*, 4(3), 915-923.

24. Ismail, M. S; Moghavvemi, M; Mahlia, T. M. I. (2013). Characterization of PV panel and global optimization of its model parameters using genetic algorithm. *Energy Conversion and Management*, 73, 10-25.

25. Jordehi, A. R. (2016a). Parameter estimation of solar photovoltaic (PV) cells: A review. *Journal of Renewable and Sustainable Energy*, 61, 354-371.

26. Jordehi, A. R. (2016b). Time varying acceleration coefficients particle swarm optimisation (TVACPSO): A new optimisation algorithm for estimating parameters of PV cells and modules. *Energy Conversion and Management*, 129, 262-274.

27. Kang, T; Yao, J; Jin, M; Yang, S; Duong, T. (2018). A novel improved cuckoo search algorithm for parameter estimation of photovoltaic (PV) models. *Energies*, 11(5), 1060.

28. Khotbehsara, A. Y; Shahhoseini, A. (2018). A fast modeling of the double-diode model for PV modules using combined analytical and numerical approach. *Solar Energy*, 162, 403-409.

29. Li, S; Gong, W; Yan, X; Hu, C; Bai, D; Wang, L; Gao, L. (2019a). Parameter extraction of photovoltaic models using an improved teaching learning-based optimization. *Energy Conversion Management*, 186, 293-305.

30. Li, S; Gong, W; Yan, X; Hu, C; Bai, D; Wang, L. (2019b). Parameter estimation of photovoltaic models with memetic adaptive differential evolution. *Solar Energy*, 190, 465-474.

31. Li, S; Gu, Q; Gong, W; Ning, B. (2020). An enhanced adaptive differential evolution algorithm for parameter extraction of photovoltaic models. *Energy Conversion Management*, 205, 112443.

32. Liao, Z; Chen, Z; Li, S. (2020). Parameters extraction of photovoltaic models using triple-phase teaching learning-based optimization. *IEEE Access*, 8, 69937-69952.

33. Lin, P; Cheng, S; Yeh, W; Chen, Z; Wu, L. (2017). Parameters extraction of solar cell models using a modified simplified swarm optimization algorithm. *Solar Energy*, 144, 594-603.

34. Long, W; Cai, S; Jiao, J; Xu, M; Wu, T. (2020). A new hybrid algorithm based on grey wolf optimizer and cuckoo search for parameter extraction of solar photovoltaic models. *Energy Conversion Management*, 203, 112243.

35. Lun, S; Du, C; Yang, G; Wang, S; Guo, T; Sang, J; Li, J. (2013a). An explicit approximate I-V characteristic model of a solar cell based on padé approximate. *Solar Energy*, 92, 147-159.

36. Lun, S; Du, C; Guo, T; Wang, S; Sang, J; Li, J. (2013b). A new explicit I-V model of a solar cell based on Taylor's series expansion. *Solar Energy*, 94, 221-232.

37. Ma, J. (2014). Optimization Approaches for Parameter Estimation and Maximum Power Point Tracking (MPPT) of Photovoltaic Systems. Ph.D. Thesis, University of Liverpool, Liverpool, UK.

38. Motahhir, S; El Hammoumi, A; El Ghzizal, A. (2018). Photovoltaic system with quantitative comparative between an improved MPPT and existing INC and P&O methods under fast varying of solar irradiation. *Energy Reports*, 4, 341-350.

39. Muhammadsharif, F. F; Hashim, S; Hameed, S. S; Ghoshal, S. K; Abdullah, I. K; Macdonald, J. E, Yahya, M. Y. (2019). Brent's algorithm based new computational approach for accurate determination of single-diode model parameters to simulate solar cells and modules. *Solar Energy*, 193, 782-798.

40. Oliva, D; Ewees, A. A; El Aziz, M. A; Hassanien, A. E; Cisneros, M. P. (2017b). A chaotic improved artificial bee colony for parameter estimation of photovoltaic cells. *Energies*, 10(7), 865.

41. Pillai, D. S; Rajasekar, N. (2018). Metaheuristic algorithms for PV parameter identification: A comprehensive review with an application to threshold setting for fault detection in PV systems. *Renewable and Sustainable Energy Reviews*, 82(Part 3), 3503-3525.

42. Pourmousa, N; Ebrahimi, S. M; Malekzadeh, M; Alizadeh, M. (2019). Parameter estimation of photovoltaic cells using improved Lozi map based chaotic optimization Algorithm. *Solar Energy*, 180, 180-191.

43. Ridha, H. M; Heidari, A. A; Wang, M; Chen, H. (2020). Boosted mutation-based Harris hawks optimizer for parameters identification of single-diode solar cell models. *Energy Conversion Management*, 209, 112660.

44. Rodrigues, E. M. G; Godina, R; Marzband, M; Pouresmaeil, E. (2018). Simulation and comparison of mathematical models of PV cells with growing levels of complexity. *Energies*, 11(11), 2902.

45. Soon, J. J; Low, K. S. (2012). Photovoltaic model identification using particle swarm

optimization with inverse barrier constraint. *IEEE Transactions on Power Electronics*, 27(9), 3975-3983.

46. Wolf, M; Noel, G. T; Stirn, R. J. (1977). Investigation of the double exponential in the current-voltage characteristics of silicon solar cells. *IEEE Transactions on Electron Devices*, 24(4), 419-428.

47. Xiong, G; Zhang, J; Yuan, X; Shi, D; He, Y. (2018). Application of symbiotic organisms search algorithm for parameter extraction of solar cell models. *Applied Sciences*, 8(11), 2155.

48. Xiong, G; Zhang, J; Shi, D; Yuan, X. (2019). Application of supply-demand-based optimization for parameter extraction of solar photovoltaic models. *Complexity*, 2019, 1-22.

49. Yang, X; Gong, W; Wang, L. (2019). Comparative study on parameter extraction of photovoltaic models via differential evolution. *Energy Conversion and Management*, 201, 112113.

50. Yu, K; Liang, J. J; Qu, B. Y; Chen, X; Wang, H. (2017a). Parameters identification of photovoltaic models using an improved JAYA optimization algorithm. *Energy Conversion and Management,* 150, 742-753.

51. Yu, K; Chen, X; Wang, X; Wang, Z. (2017b). Parameters identification of photovoltaic models using self-adaptive teaching-learning-based optimization. *Energy Conversion and Management*, 145, 233-246.

52. Yu, K; Qu, B; Yue, C; Ge, S; Chen, X; Liang, J. (2019). A performance-guided JAYA algorithm for parameters identification of photovoltaic cell and module. *Applied Energy*, 237, 241-257.

53. Zhang, Y; Lin, P; Chen, Z; Cheng, S. (2016). A population classification evolution algorithm for the parameter extraction of solar cell models. International Journal of Photoenergy, 2016, 2174573.

54. Zhu, Y; Lian, W; Lu, L; Kamunyu, P; Yu, C; Dai, S; Hu, Y. (2017). Online modelling and calculation for operating temperature of silicon-based PV bodules based on BP-ANN. *International Journal of Photoenergy*, 2017, 6759295.

Table 1. *Error functions for SDM, DDM, and PMM*

Model	$f(V, I, \emptyset)$	$\emptyset$
SDM	$I - \left(I_{PV} - I_O\left\{\exp\left[\frac{(V+IR_S)}{AV_{TH}}\right] - 1\right\} - \frac{V+IR_S}{R_P}\right)$	$\{I_{PV}, I_O, R_S, R_P, A\}$
DDM	$I - \left(I_{PV} - I_{O1}\left\{\exp\left[\frac{(V+IR_S)}{A_1V_{TH}}\right] - 1\right\} - I_{O2}\left\{\exp\left[\frac{(V+IR_S)}{A_2V_{TH}}\right] - 1\right\} - \frac{V+IR_S}{R_P}\right)$	$\{I_{PV}, I_{O1}, I_{O2}, R_S, R_P, A_1, A_2\}$
PMM	$I - \left(I_{PVM} - I_{\mathrm{OM}}\left\{\exp\left[\frac{(V+IR_{SM})}{A_MV_{TH}}\right] - 1\right\} - \frac{V+IR_{SM}}{R_{PM}}\right)$	$\{I_{PVM}, I_{OM}, R_{SM}, R_{PM}, A_M\}$

Algorithm 1. *Pseudocode of TADE*

1. Input values of *D* and *NP*
2. Define vector x_{min} and x_{max}
3. Randomly generate a population of individuals by using Equation (18)
4. **while** termination criteria *NFE* < *MNFE* **do**
5. Evaluate the population to obtain the best candidates that satisfy the *RMSE*
6. Adapt control parameters $F_i^{(G)}$ and $CR_i^{(G)}$ as per Equations (20), (21), and (22)
7. Perform mutation to generate mutant individuals $v_{i,j}^{(G)}$ as per Equation (23)
8. Perform crossover to generate trial individuals $t_{i,j}^{(G)}$ as per Equation (24)
9. Select the best fitness values and individuals for next-generation $x_{i,j}^{(G+1)}$ using Equation (25).
10. Update the population for the next generation with Equation (27)
11. Increase the counter *G* = *G* +1
12. end **while** loop
13. Postprocess results and visualization

Table 2. *Comparison of the RTC-France PV cell (SDM)*

	IJAYA	SATLBO	TLABC	GWOCS	DE	TADE
I_{PV} (A)	0.7608	0.7608	0.7608	0.7608	0.7608	0.7608
I_O (μA)	0.3228	0.3232	0.3230	0.3219	0.3230	0.3230
R_S (Ω)	0.0364	0.0363	0.0364	0.0364	0.0364	0.0364
R_P (Ω)	53.7595	53.7256	53.7164	53.6320	53.7185	53.7185
A	1.4811	1.4812	1.4812	1.4808	1.4812	1.4812
Best	9.8603×10^{-04}	9.8602×10^{-04}	9.8602×10^{-04}	9.8607×10^{-04}	9.8602×10^{-04}	9.8602×10^{-04}
Worst	1.0622×10^{-03}	9.9494×10^{-03}	1.0397×10^{-03}	9.9095×10^{-04}	1.5686×10^{-03}	9.8979×10^{-04}
Mean	9.9204×10^{-03}	9.8780×10^{-04}	9.9852×10^{-04}	9.8874×10^{-04}	1.1224×10^{-03}	9.8687×10^{-04}
SD	1.4000×10^{-05}	2.3000×10^{-06}	1.8602×10^{-05}	2.4696×10^{-06}	1.3800×10^{-04}	1.3448×10^{-06}
MNFE	50000	50000	50000	50000	20000	10000

Table 3. *Estimated RMSE of the RTC-France PV cell (SDM) by different algorithms*

Ref.	Algorithm	RMSE
Proposed	TADE	9.860219×10^{-04}
Liao *et al.*, 2020	TPTLBO	9.8602×10^{-04}
Xiong *et al.*, 2019	SDO	9.8602×10^{-04}
Yu *et al.*, 2019	PGJAYA	9.8602×10^{-04}
Ćalasan *et al.*, 2019	COA	9.860221×10^{-04}
Pourmousa *et al.*, 2019	ILCOA	9.86021×10^{-04}
Li *et al.*, 2019a	ITLBO	9.8602×10^{-04}
Li, *et al.*, 2019b	MADE	9.8602×10^{-04}
Beigi and Maroosi, 2018	HFAPS	9.8602×10^{-04}
Kang *et al.*, 2018	ImCSA	9.8602×10^{-04}
Gao *et al.*, 2018	ISCE	9.860219×10^{-04}
Xiong *et al.*, 2018	SOS	9.8609×10^{-04}
Chen *et al.*, 2018a	pSFS	9.8602×10^{-04}
Lin *et al.*, 2017	MSSO	9.8607×10^{-04}
Chen *et al.*, 2017	BLPSO	11.239×10^{-04}
Oliva *et al.*, 2017	CIABC	9.8602×10^{-04}
Zhang *et al.*, 2016	PCE	9.86022×10^{-04}

Table 4. *Estimated results of the RTC-France PV cell (SDM) obtained using TADE*

Item	Measured		Estimated *I*		Estimated *P*	
	***V* (Volt)**	***I* (Ampere)**	I_{est} **(Ampere)**	***IAE***	P_{est} **(Watt)**	***IAE***
1	-0.2057	0.7640	0.76408770	0.00008770	-0.15717284	0.00001804
2	-0.1291	0.7620	0.76266309	0.00066309	-0.09845980	0.00008560
3	-0.0588	0.7605	0.76135531	0.00085531	-0.04476769	0.00005029
4	0.0057	0.7605	0.76015399	0.00034601	0.00433288	0.00000197
5	0.0646	0.7600	0.75905521	0.00094479	0.04903497	0.00006103
6	0.1185	0.7590	0.75804234	0.00095766	0.08982802	0.00011348
7	0.1678	0.7570	0.75709165	0.00009165	0.12703998	0.00001538
8	0.2132	0.7570	0.75614136	0.00085864	0.16120934	0.00018306
9	0.2545	0.7555	0.75508687	0.00041313	0.19216961	0.00010514
10	0.2924	0.7540	0.75366388	0.00033612	0.22037132	0.00009828
11	0.3269	0.7505	0.75139097	0.00089097	0.24562971	0.00029126
12	0.3585	0.7465	0.74735385	0.00085385	0.26792636	0.00030611
13	0.3873	0.7385	0.74011722	0.00161722	0.28664740	0.00062635
14	0.4137	0.7280	0.72738223	0.00061777	0.30091803	0.00025557
15	0.4373	0.7065	0.70697265	0.00047265	0.30915914	0.00020669
16	0.4590	0.6755	0.67528015	0.00021985	0.30995359	0.00010091
17	0.4784	0.6320	0.63075827	0.00124173	0.30175476	0.00059404

18	0.4960	0.5730	0.57192836	0.00107164	0.28367647	0.00053153
19	0.5119	0.4990	0.49960702	0.00060702	0.25574883	0.00031073
20	0.5265	0.4130	0.41364879	0.00064879	0.21778609	0.00034159
21	0.5398	0.3165	0.31751011	0.00101011	0.17139196	0.00054526
22	0.5521	0.2120	0.21215494	0.00015494	0.11713074	0.00008554
23	0.5633	0.1035	0.10225131	0.00124869	0.05759816	0.00070339
24	0.5736	-0.0100	-0.00871754	0.00128246	-0.00500038	0.00073562
25	0.5833	-0.1230	-0.12550741	0.00250741	-0.07320847	0.00146257
26	0.5900	-0.2100	-0.20847233	0.00152767	-0.12299867	0.00090133
RMSE						0.00098602

Table 5. *Comparison of the RTC-France PV cell (DDM)*

	IJAYA	**SATLBO**	**TLABC**	**GWOCS**	**DE**	**TADE**
I_{PV} (A)	0.7601	0.7608	0.7608	0.76076	0.7608	0.7608
I_{O1} (μA)	0.0050	0.2509	0.4239	0.53772	0.3756	0.5798
I_{O2} (μA)	0.7509	0.5454	0.2401	0.24855	0.2715	0.2624
R_S (Ω)	0.0376	0.0366	0.0367	0.03666	0.0366	0.0369
R_P (Ω)	77.8519	55.1170	54.6680	54.7331	54.5704	54.8885
A_1	1.2186	1.4598	1.9075	2.0000	1.9999	2.0685
A_2	1.6247	1.9994	1.4567	1.4588	1.4664	1.4632
Best	$9.8293x10^{-04}$	$9.8280x10^{-04}$	$9.8415x10^{-04}$	$9.8334x10^{-04}$	$9.8344x10^{-04}$	$9.8243x10^{-04}$
Worst	$1.4055x10^{-03}$	$1.0470x10^{-03}$	$1.5048x10^{-03}$	$1.0017x10^{-03}$	$1.4490x10^{-03}$	$9.9664x10^{-04}$
Mean	$1.0269x10^{-03}$	$9.9811x10^{-04}$	$1.0555x10^{-03}$	$9.9411x10^{-04}$	$1.0150x10^{-03}$	$9.8730x10^{-04}$
SD	$9.8300x10^{-05}$	$1.9500x10^{-05}$	$1.5503x10^{-04}$	$9.5937x10^{-06}$	$7.8100x10^{-05}$	$2.4831x10^{-06}$
MNFE	50000	50000	50000	50000	30000	20000

Table 6. *Estimated RMSE of the RTC-France PV cell (DDM) by different algorithms*

Ref.	**Algorithm**	**RMSE**
Proposed	TADE	$9.824321x10^{-04}$
Liao *et al.*, 2020	TPTLBO	$9.8248x10^{-04}$
Xiong *et al.*, 2019	SDO	$9.8250x10^{-04}$
Yu *et al.*, 2019	PGJAYA	$9.8263x10^{-04}$
Li *et al.*, 2019a	ITLBO	$9.8248x10^{-04}$
Li, *et al.*, 2019b	MADE	$9.8261x10^{-04}$
Beigi and Maroosi, 2018	HFAPS	$9.8248x10^{-04}$
Kang *et al.*, 2018	ImCSA	$9.8249x10^{-04}$
Gao *et al.*, 2018	ISCE	$9.824849x10^{-04}$
Xiong *et al.*, 2018	SOS	$9.8518x10^{-04}$
Chen *et al.*, 2018a	pSFS	$9.8255x10^{-04}$
Lin *et al.*, 2017	MSSO	$9.8281x10^{-04}$
Chen *et al.*, 2017	BLPSO	$11.042x10^{-04}$
Oliva *et al.*, 2017	CIABC	$9.8262x10^{-04}$

Zhang *et al.*, 2016	PCE	$9.8248x10^{-04}$

Table 7. *Estimated results of the RTC-France PV cell (DDM) obtained using TADE*

Item	Measured		Estimated *I*		Estimated *P*	
	***V* (Volt)**	***I* (Ampere)**	**I_{est} (Ampere)**	**IAE**	**P_{est} (Watt)**	***IAE***
1	-0.2057	0.7640	0.76401767	0.00001767	-0.15715844	0.00000364
2	-0.1291	0.7620	0.76262337	0.00062337	-0.09845468	0.00008048
3	-0.0588	0.7605	0.76134325	0.00084325	-0.04476698	0.00004958
4	0.0057	0.7605	0.76016689	0.00033311	0.00433295	0.00000190
5	0.0646	0.7600	0.75908981	0.00091019	0.04903720	0.00005880
6	0.1185	0.7590	0.75809445	0.00090555	0.08983419	0.00010731
7	0.1678	0.7570	0.75715526	0.00015526	0.12705065	0.00002605
8	0.2132	0.7570	0.75620793	0.00079207	0.16122353	0.00016887
9	0.2545	0.7555	0.75514501	0.00035499	0.19218440	0.00009035
10	0.2924	0.7540	0.75370046	0.00029954	0.22038201	0.00008759
11	0.3269	0.7505	0.75139440	0.00089440	0.24563083	0.00029238
12	0.3585	0.7465	0.74731819	0.00081819	0.26791357	0.00029332
13	0.3873	0.7385	0.74004752	0.00154752	0.28662040	0.00059935
14	0.4137	0.7280	0.72729568	0.00070432	0.30088222	0.00029138
15	0.4373	0.7065	0.70689623	0.00039623	0.30912572	0.00017327
16	0.4590	0.6755	0.67523883	0.00026117	0.30993462	0.00011988
17	0.4784	0.6320	0.63076307	0.00123693	0.30175705	0.00059175
18	0.4960	0.5730	0.57197238	0.00102762	0.28369830	0.00050970
19	0.5119	0.4990	0.49966913	0.00066913	0.25578063	0.00034253
20	0.5265	0.4130	0.41369849	0.00069849	0.21781226	0.00036776
21	0.5398	0.3165	0.31752601	0.00102601	0.17140054	0.00055384
22	0.5521	0.2120	0.21212636	0.00012636	0.11711496	0.00006976
23	0.5633	0.1035	0.10218829	0.00131171	0.05756266	0.00073889
24	0.5736	-0.0100	-0.00876745	0.00123255	-0.00502901	0.00070699
25	0.5833	-0.1230	-0.12552567	0.00252567	-0.07321912	0.00147322
26	0.5900	-0.2100	-0.20839585	0.00160415	-0.12295355	0.00094645
RMSE						0.00098243

Table 8. *Comparison of the Photowatt-PWP 201 PV module*

	IJAYA	SATLBO	TLABC	GWOCS	DE	TADE
I_{PVM} (A)	1.0305	1.0305	1.0306	1.03049	1.0305	1.0305
I_{OM} (μA)	3.4703	3.4827	3.4715	3.465	3.4823	3.4823
R_{SM} (Ω)	1.2016	1.2013	1.2017	1.2019	1.2013	1.2013
R_{PM} (Ω)	977.3752	982.4038	972.9357	982.7566	981.9819	981.9823
A_M	48.6298	48.6433	48.6313	48.62367	48.6428	48.6428

Best	$2.4251x10^{-03}$	$2.4251x10^{-03}$	$2.4251x10^{-03}$	$2.4251x10^{-03}$	$2.4251x10^{-03}$	$2.4251x10^{-03}$
Worst	$2.4393x10^{-03}$	$2.4291x10^{-03}$	$2.4458x10^{-03}$	$2.4275x10^{-03}$	$2.4384x10^{-03}$	$2.4268x10^{-03}$
Mean	$2.4251x10^{-03}$	$2.4254x10^{-03}$	$2.4265x10^{-03}$	$2.4261x10^{-03}$	$2.4259x10^{-03}$	$2.4251x10^{-03}$
SD	$3.7800x10^{-06}$	$7.4100x10^{-07}$	$3.9957x10^{-06}$	$1.1967x10^{-06}$	$2.7000x10^{-06}$	$5.2004x10^{-07}$
MNFE	50000	50000	50000	50000	10000	10000

Table 9. *Estimated RMSE of the Photowatt-PWP201 PV module by different algorithms*

Ref.	Algorithm	RMSE
proposed	TADE	$2.425075x10^{-03}$
Liao *et al.*, 2020	TPTLBO	$2.4251x10^{-03}$
Yu *et al.*, 2019	PGJAYA	$2.425075x10^{-03}$
Li *et al.*, 2019a	ITLBO	$2.4251x10^{-03}$
Li, *et al.*, 2019b	MADE	$2.425x10^{-03}$
Xiong *et al.*, 2018	SOS	$2.4251x10^{-03}$
Kang *et al.*, 2018	ImCSA	$2.425x10^{-03}$
Jordehi, 2016b	TVACPSO	$6.9665x10^{-03}$

Table 10. *Estimated results of the Photowatt-PWP 201 PV module obtained using TADE*

Item	Measured		Estimated *I*		Estimated *P*	
	***V* (Volt)**	***I* (Ampere)**	I_{est} **(Ampere)**	***IAE***	P_{est} **(Watt)**	***IAE***
1	0.1248	1.0315	1.02911916	0.00238084	0.12843407	0.00029713
2	1.8093	1.0300	1.02738107	0.00261893	1.85884058	0.00473842
3	3.3511	1.0260	1.02574180	0.00025820	3.43736334	0.00086526
4	4.7622	1.0220	1.02410715	0.00210715	4.87700309	0.01003469
5	6.0538	1.0180	1.02229180	0.00429180	6.18875013	0.02598173
6	7.2364	1.0155	1.01993068	0.00443068	7.38062638	0.03206218
7	8.3189	1.0140	1.01636311	0.00236311	8.45502304	0.01965844
8	9.3097	1.0100	1.01049615	0.00049615	9.40741602	0.00461902
9	10.2163	1.0035	1.00062897	0.00287103	10.22272574	0.02933131
10	11.0449	0.9880	0.98454838	0.00345162	10.87423839	0.03812281
11	11.8018	0.9630	0.95952168	0.00347832	11.32408292	0.04105048
12	12.4929	0.9255	0.92283882	0.00266118	11.52893307	0.03324588
13	13.1231	0.8725	0.87259966	0.00009966	11.45121263	0.00130788
14	13.6983	0.8075	0.80727426	0.00022574	11.05828504	0.00309221
15	14.2221	0.7265	0.72833648	0.00183648	10.35847422	0.02611857
16	14.6995	0.6345	0.63713800	0.00263800	9.36561003	0.03877728
17	15.1346	0.5345	0.53621306	0.00171306	8.11537022	0.02592652
18	15.5311	0.4275	0.42951132	0.00201132	6.67078334	0.03123809
19	15.8929	0.3185	0.31877448	0.00027448	5.06625098	0.00436233
20	16.2229	0.2085	0.20738951	0.00111049	3.36445923	0.01801542

21	16.5241	0.1010	0.09616717	0.00483283	1.58907597	0.07985813
22	16.7987	-0.0080	-0.00832539	0.00032539	-0.13985566	0.00546606
23	17.0499	-0.1110	-0.11093648	0.00006352	-1.89145593	0.00108297
24	17.2793	-0.2090	-0.20924727	0.00024727	-3.61564628	0.00427258
25	17.4885	-0.3030	-0.30086359	0.00213641	-5.26165284	0.03736266
RMSE						0.00242507

Table 11. *Estimated results for the KC200GT PV module at different irradiance and temperature obtained using TADE*

	Irradiance, Temperature						
	200 W/m², 25℃	**400 W/m², 25℃**	**600 W/m², 25℃**	**800 W/m², 25℃**	**1000 W/m², 25℃**	**1000 W/m², 50℃**	**1000 W/m², 75℃**
I_{PVM} (A)	1.57569399	3.24498143	4.88010408	6.53597163	8.19970756	8.23783237	8.35619048
I_{OM} (μA)	0.01783577	0.00889579	0.00751949	0.00024648	0.00005773	2.36019426	0.10624394
R_{SM} (Ω)	65.548458	62.590896	62.265731	53.080513	50.274351	71.148817	49.346298
R_{PM} (Ω)	0.84520850	0.39610901	0.32958665	0.31117124	0.28686157	0.14227928	0.33271560
A_M	124077.3595	349.256060	256.428075	153.274461	109.561569	224.722903	101.771266
Best	$7.455108x10^{-03}$	$1.293504x10^{-02}$	$2.702622x10^{-02}$	$2.275030x10^{-02}$	$1.179859x10^{-02}$	$6.527374x10^{-02}$	$3.768100x10^{-02}$
Worst	$7.498053x10^{-03}$	$1.294912x10^{-02}$	$2.739434x10^{-02}$	$2.299584x10^{-02}$	$1.199074x10^{-02}$	$6.549381x10^{-02}$	$3.788584x10^{-02}$
Mean	$7.471488x10^{-03}$	$1.293808x10^{-02}$	$2.708569x10^{-02}$	$2.288880x10^{-02}$	$1.183797x10^{-02}$	$6.537953x10^{-02}$	$3.773224x10^{-02}$
SD	$1.303167x10^{-05}$	$4.587912x10^{-06}$	$1.004395x10^{-04}$	$7.942290x10^{-05}$	$4.985857x10^{-05}$	$7.861897x10^{-05}$	$6.353135x10^{-05}$
MNFE	10000	10000	10000	10000	10000	10000	10000

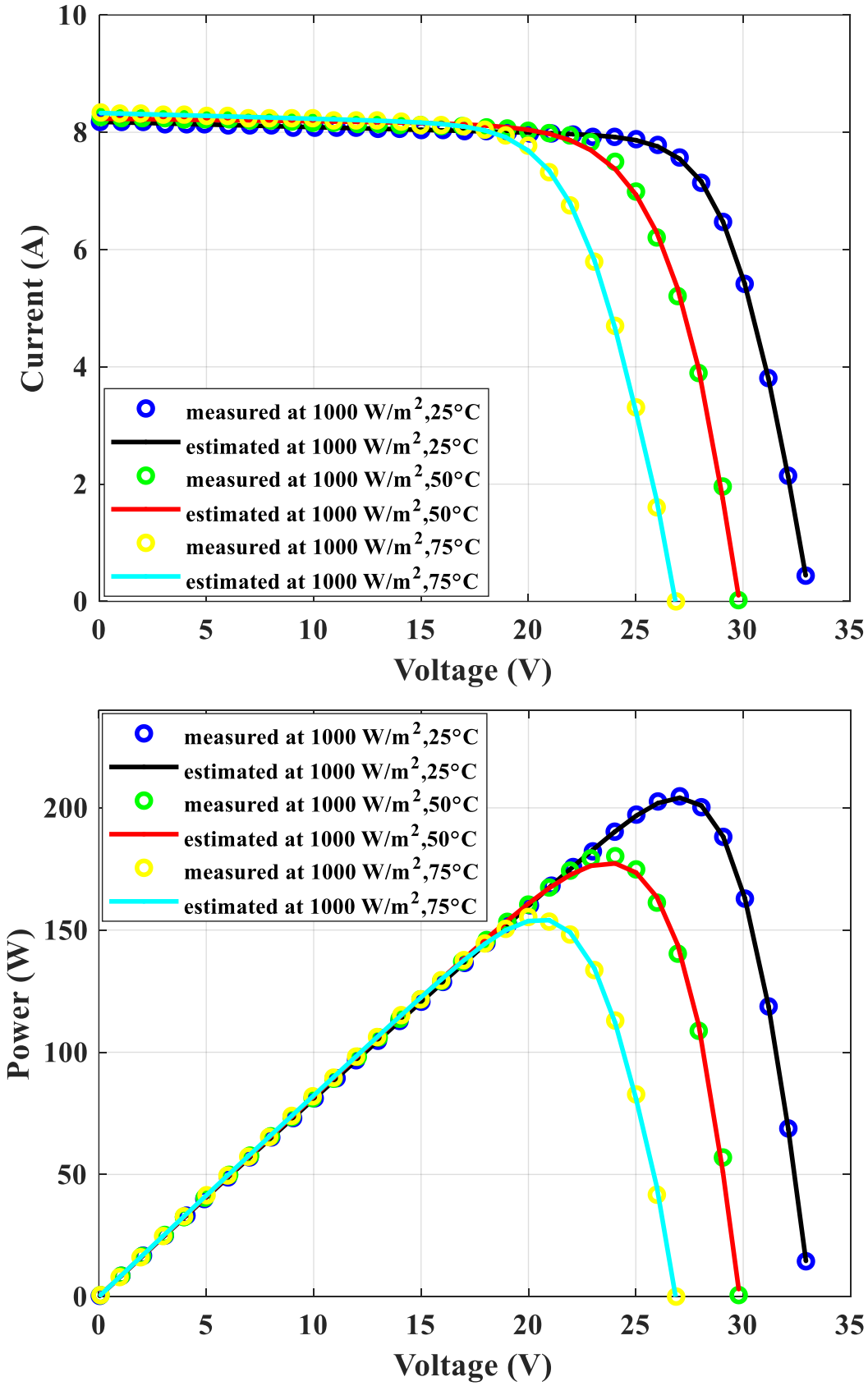

Figure 12. *Estimated and measured data of the KC200GT PV module under various temperature levels*